ECT and LS-SVM Based Void Fraction Measurement of Oil-Gas Two-Phase Flow

Peng, Zhenrui*[+]; Yin, Hong

School of Mechatronics Engineering, Lanzhou Jiaotong University, Lanzhou 730070, CHINA

ABSTRACT: *A method based on Electrical Capacitance Tomography (ECT) and an improved Least Squares Support Vector Machine (LS-SVM) is proposed for void fraction measurement of oil-gas two-phase flow. In the modeling stage, to solve the two problems in LS-SVM, pruning skills are employed to make LS-SVM sparse and robust; then the Real-Coded Genetic Algorithm is introduced to solve the difficult problem of parameters selection in LS-SVM then. In the measurement process, the flow pattern of oil-gas two-phase flow is identified by using fast back-projection image reconstruction and a fuzzy pattern recognition technique and the void fraction is computed using the void fraction model corresponding to the identified flow pattern. Experimental results demonstrate that both the improvement of LS-SVM and the parameter optimization are effective. The results also show that the real-time performance of the proposed void fraction measurement method is good, and the measurement precision can satisfy the application requirement.*

KEY WORDS: *Void fraction, Two-phase flow, Electrical Capacitance Tomography (ECT), Least Squares Support Vector Machine (LS-SVM), Real-Coded Genetic Algorithm (RC-GA).*

INTRODUCTION

Two-phase flow exists widely in industries such as chemical, petroleum and power. Void fraction is one of the important parameters of oil-gas two-phase flow. The on-line void fraction measurement is of great importance for safety, environmental protection and energy conservation in industry. However, the flow characteristics of two-phase flow are far more complicated than those of single phase flow, owing to the phase interface and relative velocity in the two-phase flow. On-line void fraction measurement has become a key problem in the two-phase flow research field and this problem has not been solved well till now [1,2].

The technology of Electrical Capacitance Tomography (ECT), with the features of simplicity, non-intrusiveness, low cost, and fast speed, has gained some achievements in the void fraction measurement of two-phase flow. However, in conventional void fraction measurement methods based on ECT, the void fraction values are estimated by the cross-sectional images of the voidage distribution of two-phase flow. A high quality image is necessary to determine the precise void fraction. While reconstructing a high quality image needs a complex and time-consuming image reconstruction algorithm, this method cannot satisfy the real-time requirement of the measurement [1,2].

Support Vector Machine (SVM), a novel machine

41

learning method with high generalization ability, developed by Vapnik and his co-workers, has been successfully used in many applications including pattern recognition, function estimation and financial time series forecasting [3-5]. Least Squares Support Vector Machine (LS-SVM), a new version of SVM, has the features of simplicity, high efficiency and quick convergence [4]. At present, some drawbacks still exist in LS-SVM. When these drawbacks are overcome, LS-SVM will be more suitable for the modeling of void fraction measurement of two-phase flow, which is essentially a function estimation problem.

The goal of the present work is to propose a new method for on-line void fraction measurement of oil-gas two-phase flow. In this method, ECT sensor is used to obtain capacitance measurement information. The flow pattern is identified by combining fast ECT image reconstruction with fuzzy pattern recognition. An improved LS-SVM is applied to establish the void fraction measurement models corresponding to different flow patterns. In the practical measurement process, the flow pattern of oil-gas two-phase flow is identified by using fast back-projection image reconstruction and fuzzy pattern recognition techniques first, and then the void fraction is computed by using the void fraction model corresponding to the identified flow pattern.

EXPERIMENTAL SECTION
Experimental Set-Up

Fig. 1 shows the void fraction measurement system, which mainly consists of a 12- electrode ECT sensor, a data acquisition and signal processing unit and a computer. In this figure, the computer is not displayed. Fig. 2 shows the 12-elcotrode capacitance sensor. Fig. 3 shows the more detailed structure of the ECT sensor, which consists of 12 electrodes mounted on the outside of an insulating pipe, projected guard electrodes, screen, and insulating pipeline. The insulating pipeline of the capacitance sensor is made of plexiglass. Its inner diameter is 50mm and its thickness 4 mm. The length of each electrode is 60mm and the width of each electrode 13.0 mm. The capacitance sensor converts the distribution of the two-phase flow medium in the pipeline to the capacitance output of the capacitance sensor [2,6].

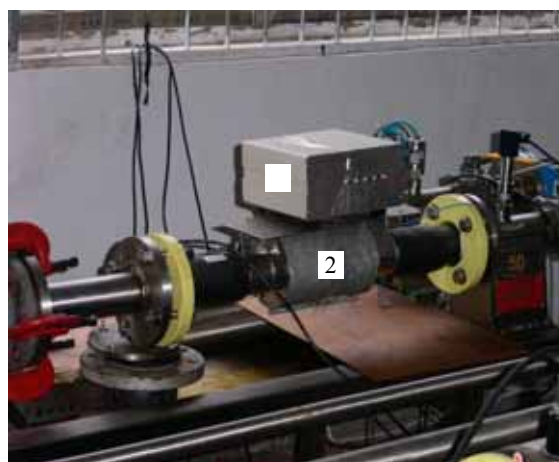Fig. 4 shows the capacitance data acquisition and signal processing unit. This unit measures the capacitance

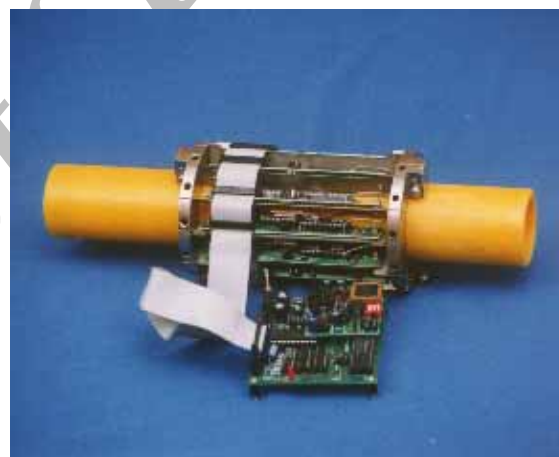***Fig. 1: Void fraction measurement system. 1- Data acquisition & signal processing unit, 2- 12- electrode ECT sensor.***
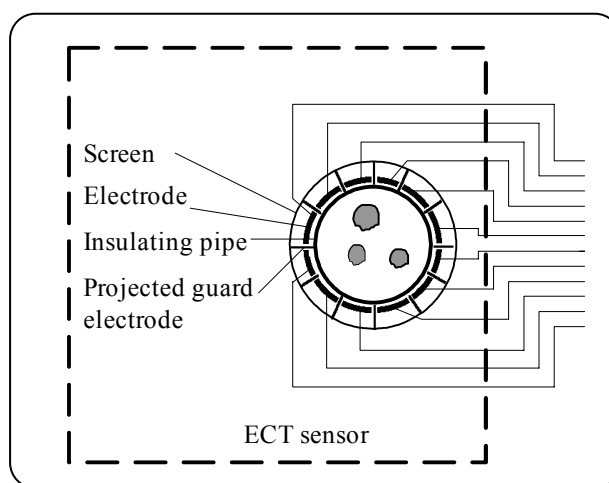

Fig. 2: 12-Elcotrode capacitance sensor.

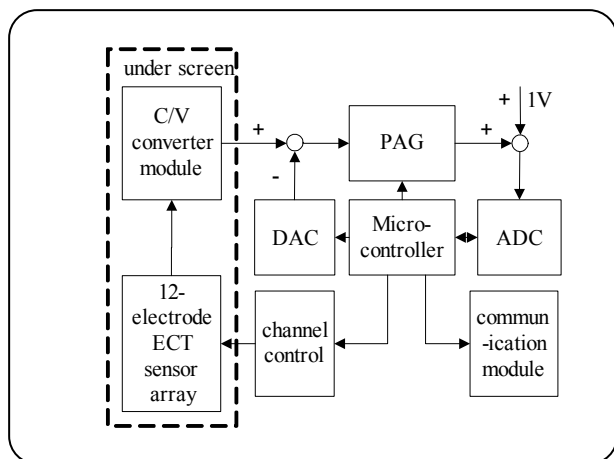***Fig. 3: Schematic diagram of 12-elcotrode capacitance sensor.***

42

Fig. 4: Schematic diagram of data acquisition & signal processing unit.

Fig. 5: Flow pattern of oil-gas two-phase flow in horizontal pipeline [1].

between all possible combination pairs of the 12 electrodes, converts the measured capacitance into a digital signal, and sends the data to the image reconstruction computer. The capacitance-to-voltage (C/V) conversion circuit (the capacitance measurement circuit) in the capacitance data acquisition and signal processing unit, has high data acquisition speed, wide dynamic range, stray-immunity, and low base-line drift [2,6].

Channel selection, output of ADC and the gain setting of PGA are controlled by a microcontroller. The results of analog-to-digital conversion are sent to the image reconstruction computer by the micro-controller via the serial communication module.

Measurement Principle

The void fraction measurement principle is as follow. Each phase (component) of two-phase flow has its own permittivity (dielectric constant), which is different from that of the other phase. The change of void fraction and its distribution leads to the alteration of equivalent permittivity of two-phase flow and further results in the variation of capacitance measurement values. By measuring the capacitance changes between all possible combination pairs of the electrodes of capacitance sensor, the change of two-phase flow void fraction and its distribution can be obtained [2]. Taking the 12-electrode ECT system as an example, there are 66 ($C_{12}^2 = 12 \times (12-1)/2 = 66$).

Capacitance measurement values between all possible combination pairs of the electrodes of capacitance sensor. Since the capacitance measurement values reflect the
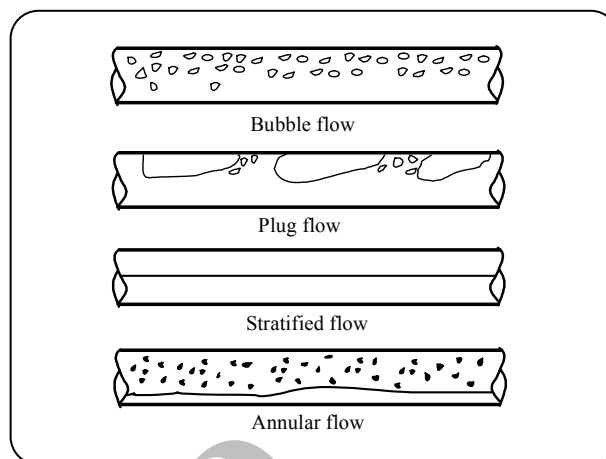
change of void fraction of two-phase flow, the void fraction value β can be essentially regarded as a function of capacitance measurements:

$$\beta = f\left(C_{1,2}, C_{1,3}, ..., C_{11,12}\right) \tag{1}$$

Due to complex relationship between permittivity and capacitance measurement values, there is no analytical solution to Eq. (1).

Flow pattern of two-phase flow is a three-dimensional flow phenomenon. There exist many kinds of flow patterns such as bubble flow, stratified flow, plug flow and annular flow as shown in Fig. 5. The flow pattern has great influence on the void fraction measurement. It is very difficult for single void fraction model to perform the void fraction measurement under different flow patterns. Meanwhile, despite the complexity of two-phase flow, the void fraction is a cross-section parameter, which represents the ratio of the gas concentration to the total gas-liquid concentration. At a certain moment, the cross-section flow pattern only takes on one of the flow patterns (stratified flow, bubble flow, and annular flow), which are shown in Fig. 6. Therefore, this work adopts the improved LS-SVM to establish void-fraction measurement model corresponding to the three cross-section flow patterns mentioned above. Thus, the influence of the flow pattern on the void fraction measurement is overcome to a great degree. The main idea for void fraction measurement in this work is shown in Fig. 7. The ECT capacitance sensor obtains the 66 capacitance values and sends them to the computer.
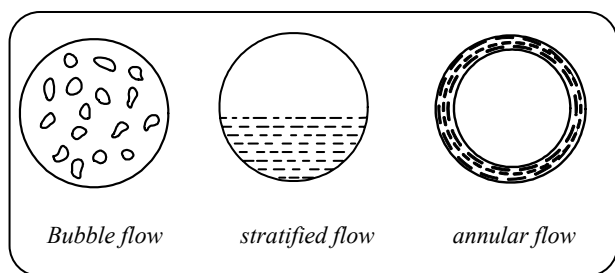
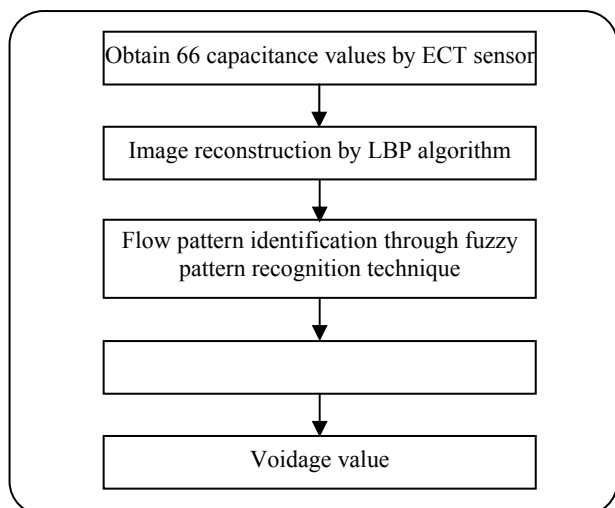**Fig. 6: Cross-section flow pattern in horizontal pipeline.**

Fig. 7: Void fraction measurement process of two-phase flow.

The linear back projection algorithm is adopted to reconstruct the cross-section image of two-phase flow in pipeline. The fuzzy pattern recognition technique is combined with the reconstructed image to identify the flow pattern (More detailed information about flow pattern identification can be found in reference [7]). The normalized capacitance measurement values are the input of the established void fraction model. The void fraction is computed using the void fraction model corresponding to the identified flow pattern. Thus, the online void fraction measurement is realized.

VOID FRACTION MEASUREMENT MODELING

In this section, a brief description of regression LS-SVM is given, followed by the improvement of LS-SVM and the Real-Coded Genetic Algorithm (RC-GA) is applied to the optimal parameter selection in LS-SVM. Then, the simulation is conducted to validate the improved LS-SVM and the proposed parameters optimization method. Finally, the modeling process for the void fraction measurement is provided in detail.

Regression LS-SVM

Support Vector Machine (SVM) has been used as a method for classification and for function approximation. In this paper, void fraction measurement is essentially a function approximation problem. SVM has the remarkable characteristics such as good generalization ability, the absence of local minima, and sparse representation of solution. Another key characteristic of SVM is that training SVM is equivalent to solving a linearly constrained quadratic programming problem so that the solution of SVM is always unique and globally optimal. Least Squares Support Vector Machine (LS-SVM), a modification of SVM, adopts the least squares linear system as its loss function and therefore solves a set of linear equations. LS-SVM also has good convergence and high precision. Hence, this method is easier to use than Vapnik's SVM (standard SVM).

Given l training data $(C_1,\beta_1),..., (C_l,\beta_l)$ where the input $C_i \in R^{66}$ is the 66 normalized capacitance values and the output $\beta_i \in R$ is the void fraction value of two-phase flow the void fraction regression problem can be represented as the regression LS-SVM form [4]:

$$\min J(w,\xi) = \frac{1}{2} w^T w + \gamma \frac{1}{2} \sum_{i=1}^{l} \xi_i^2 \qquad (2)$$

subject to

$$\beta_i = w^T \varphi(C_i) + b + \xi_i \quad , \quad i = 1,2...,l \qquad (3)$$

Where J is the risk function or object function; $\varphi(\cdot)$ represents a high dimensional feature space, which is nonlinearly mapped from the input space; γ is the regularization parameter; $\xi = (\xi_1, \xi_2,...,\xi_l)$ is the error vector; w and b are weight vector and bias term, respectively.

Construct the Lagrangian

$$L(w,b,\xi,\alpha) = J(w,b,\xi) - \qquad (4)$$

$$\sum_{i=1}^{l} \alpha_i \left\{ w^T \varphi(C_i) + b - \beta_i + \xi_i \right\}$$

where $\alpha_i \in R$ is the Lagrange multiplier, which can be positive or negative in the LS-SVM formulation. From the optimization conditions, the following equations must be satisfied:

$$\begin{cases} \dfrac{\partial L}{\partial w} = 0 \rightarrow w = \sum_{i=1}^{l} \alpha_i \varphi(C_i) \\[2mm] \dfrac{\partial L}{\partial b} = 0 \rightarrow \sum_{i=1}^{l} \alpha_i = 0 \\[2mm] \dfrac{\partial L}{\partial \xi_i} = 0 \rightarrow \alpha_i = \gamma \xi_i \\[2mm] \dfrac{\partial L}{\partial \alpha_i} = 0 \rightarrow w^T \varphi(C_i) + b - \beta_i + \xi_i = 0 \end{cases} \quad (5)$$

With i=1,2,3,...,l. Eliminating w and ξ, the following matrix equation is obtained:

$$\begin{pmatrix} 0 & l_v^T \\ l_v & \Omega + \dfrac{1}{\gamma} I \end{pmatrix} \begin{bmatrix} b \\ \alpha \end{bmatrix} = \begin{bmatrix} 0 \\ \beta \end{bmatrix} \quad (6)$$

Where $\beta=[\beta_1,..., \beta_l]$ is the void fraction vector, with $l_v=[1,...,1]$, $\alpha=[\alpha_1,..., \alpha]$. Mercer's condition is applied within the matrix Ω:

$$\Omega_{ij} = \beta_i \beta_j \varphi(C_i)^T \varphi(C_j) = \beta_i \beta_j K(C_i, C_j) \quad (7)$$

Where $K(C_i, C_j)$ is a Kernel function satisfying Mercer's conditions. There are several Kernel functions such as linear Kernel function, polynomial Kernel function and radial Kernel function (RBF). These typical Kernel functions are listed in Table 1.

So far, the LS-SVM void fraction regression model is constructed as:

$$\beta(C) = \sum_{i=1}^{l} \alpha_i K(C, C_i) + b \quad (8)$$

Improvement of LS-SVM

As mentioned above, LS-SVM outperforms the standard SVM. But LS-SVM also has two drawbacks.

First, LS-SVM lacks sparsity. Compared with Vapnik's SVM, the sparseness is lost in the LS-SVM case. SVM has the sparseness characteristic in the sense that many α_l values are equal to zero. This is not the case in the LS-SVM because $\alpha_i = \gamma \xi_i$ from the optimization conditions. *Suykens et al.* [8] proposed a pruning procedure for LS-SVM: discard a relative number of the least meaningful data points, whose corresponding coefficients α_i are set to zero; re-estimate the LS-SVM and "sparse" LS-SVM is obtained.

Table 1: Typical Kernel functions.

Kernel function	Expression
Linear Kernel	$C_i^T C$
Polynomial Kernel	$\left(1 + C_i^T C\right)^d$
RBF Kernel	$\exp\left(-\|C - C_i\|^2 / \sigma^2\right)$

Second, LS-SVM has poor robustness. When LS-SVM is applied to practical industrial applications, many distribution factors must be considered, since these factors may contaminate the measurement data, and even result in outliers. If these outliers exist in the LS-SVM model, the model will have poor robustness and deteriorating generalization ability. Usually, the data points, if seriously polluted by noise, may have relative large α_i values (support values). If these α_i values are involved in an LS-SVM model, large training errors are inevitably produced and the generalization performance of LS-SVM is greatly limited.

Therefore, an easy pruning method is put forward to impose sparseness on LS-SVM. The pruning procedure is: discard data points with either very large or relative small errors; re-estimate the LS-SVM model using the data points remaining so that a more "sparse" LS-SVM is obtained. The steps are set out in more detail below.

STEP1: Set l the number of training data and k the number of testing data.

STEP2: Given l training data, determine the parameters (regulation parameter γ and Kernel parameter(s) such as σ^2 corresponding to the RBF Kernel function) in LS-SVM; obtain the LS-SVM model and evaluate the generalization performance of LS-SVM through k testing data. The generalization performance is evaluated using the following metric, namely, the Mean Square Error (MSE):

$$MSE = \frac{1}{k-1} \sum_{i=1}^{k} \left(y_i - f(x_i)\right)^2 \quad (9)$$

where y_i denotes the actual value and $f(x_i)$ denotes the regression value from LS-SVM model.

$$e_i = \frac{|y_i - f(x_i)|}{y_i} \times 100\% \quad , \quad i = 1, 2, ..., l \quad (10)$$

45

STEP4: Sort all the e_i; discard m data points corresponding to too small relative errors and n data points corresponding to too large relative errors.

STEP5: Retain l-m-n data points and set l⇐l-m-n.

STEP6: Go back to STEP1 and re-train LS-SVM on the reduced training data set, unless the MSE degrades.

RC-GA based parameters selection

The problem of parameter selection in SVM is encountered while using SVM. The training errors and generalization performance of SVM are directly affected by the selected parameters. The selection of the Kernel function and its parameters directly influences the generalization performance of LS-SVM, i.e. the precision of void fraction measurement in our context. However, it is difficult to select the proper parameters (Kernel parameters and regulation parameter) in LS-SVM. Therefore, many scholars do some research to solve the difficult problem of parameters selection. However, the grid-search method, which is time-consuming and laborious, is still preferred in practice [9]. This is only suitable for selection of few parameters selection because this approach does not perform well when more than three parameters are involved. Genetic Algorithm (GA) has greatly global search ability in optimization problem. We can regard the parameters selection in LS-SVM as an optimization problem. So it is potentially useful for us to use GA as a LS-SVM parameter optimization tool. Real-Coded Genetic Algorithm (RC-GA) offers advantages over the commonly used binary GA - it has a stronger searching ability; the coding is closer to the natural description of the problem; it does not need to convert from chromosome to phenotypes. So the efficiency of GA is increased [10]. Hence, in this paper, the LS-SVM parameters selection is regarded as an optimization problem and RC-GA is employed to search for the LS-SVM optimal parameters. Using the LS-SVM with the RBF Kernel function as an example, LS-SVM has regulation parameter γ and Kernel function parameter σ^2. The parameter optimization problem can described as:

$$\min f\left(\gamma, \sigma^2\right) = \min (MSE) \qquad (11)$$

$$\text{Subject to} \begin{cases} \gamma_{lower} \leq \gamma \leq \gamma_{upper} \\ \sigma^2_{lower} \leq \sigma^2 \leq \sigma^2_{upper} \end{cases} \qquad (12)$$

The procedure for LS-SVM parameter optimization is described in more detail below.

STEP1: Set l the number of training data and k the number of testing data. The training data determine the improved LS-SVM model, while the testing data evaluate generalization performance.

STEP2: Set the initial parameters: the maximum generation max_gen, the number of individual in the initial population numJind, crossover probability P_c, mutation probability P_m, generation counter gen_counter, generation error ε.

STEP3: Randomly generate num_ind individuals (The chromosome is composed of γ and σ^2) to constitute the initial population and employ real coding.

STEP4: Train the improved LS-SVM model and compute the individual generalization performance metric MSE (i), i=1,2,…,k.

STEP5: If the termination criterion is satisfied, go to STEP7. Otherwise, set gen-counter⇐gen-counter+1 and go to STEP6.

STEP6: Select an individual by employing the stochastic universal method; employ crossover and mutation operators to generate a new population; convert MSE (i), i=1,2,…,k to the individual fitness; go back to STEP4.

STEP7: Determine the optimal parameters combination (γ, σ^2), which corresponds to the individual with min (MSE (i)), i=1,2,…,k.

Since the GA is a stochastic search algorithm, it is difficult to formally specify convergence criteria as for the gradient method. As the fitness of a population may remain static for a number of generations before a superior individual is found, the application of conventional termination criteria becomes problematic. Hence, in this context RC-GA is terminated either after a pre-specified number of generations max_genor after min (MSE) < ε (Because the fitness function is computed through the linear transform of min (MSE), min (MSE) corresponds to the fitness value of the fittest individual).

Simulation validation for the improved LS-SVM and RC-GA parameter optimization method

To validate the success of the improvement of LS-SVM and the effectiveness of the RC-GA method for LS-SVM parameters optimization, simulations were conducted in MATLAB 7.1. MSE of the testing data was used as the generalization ability index of LS-SVM.

Table 2: MSE comparison between two LS-SVMs when no outlier exists.

No	Original LS-SVM	Improved LS-SVM
1	0.00898	0.00708
2	0.04821	0.04517
3	0.07699	0.07509
4	1.63071	1.47484

Table 3: MSE comparison between two LS-SVMs when outliers exist.

No	Original LS-SVM	Improved LS-SVM
1	0.00898	0.00708
2	0.04821	0.04517
3	0.10905	0.07713
4	5.02067	1.90825

In our study, four functions were considered. The first is the since function:

$$y = \sin c(x) = \frac{\sin(x)}{x} + \xi \quad , \quad x \in [-10, 10] \tag{13}$$

This function is often used in the literature: [3, 4, 8].

The second function has also been used in the literature [11] and is defined as:

$$y(x) = 10.391\big((x_1 - 0.4)(x_2 - 0.5) + 0.36\big) + \xi \tag{14}$$

with $x_1 \in [0,1]$, $x_2 \in [0,1]$

The third function has also been used in the literature [11] and is defined as:

$$y(x) = 1.9 \times \tag{15}$$
$$\Big(1.35 + e^{x_1} \sin\big(13(x_1 - 0.6)^2\big) \times e^{-x_2} \sin(7x_2)\Big) + \xi$$

with $x_1 \in [0,1]$, $x_2 \in [0,1]$

The fourth function has also been used in the literature [12] and is defined as:

$$y(x) = 10 \sin(\pi x_1 x_2) + 20(x_3 - 0.5) + 10x_4 + 5x_5 + \xi \tag{16}$$

with $x_1 \in [0,1]$, $x_2 \in [0,1]$

For each of the four functions above, the normally distributed noise ξ is added in the same way as in the corresponding literature. For each function, within the variable interval, 300 data points are generated from the function randomly. Among these data points, 270 data points, which are randomly selected, constitute the training data set. The other 30 data points constitute the testing data set.

First, the generalization ability between the improved LS-SVM and the original LS-SVM is compared when no outlier exists. Table 2 lists the MSEs of the original LS-SVM and the improved LS-SVM.

From Table 2, the MSEs in the improved LS-SVM are less than those in the original LS-SVM, which indicates that the improved LS-SVM helps to increase the generalization ability.

Then, the generalization ability between the improved LS-SVM and the original LS-SVM is compared when outliers exist. Outliers in training data set are created in the same way as those in literature [4]. Table 3 lists MSEs of the original LS-SVM and the improved LS-SVM, respectively.

From Table 3, after adding outliers, the MSEs in the improved LS-SVM are reduced to a great extent, which further indicates that the improvement is effective. It also shows that the improvement can eliminate the outliers as well as help to increase the generalization ability and robustness of LS-SVM.

Void fraction measurement modeling

Different Kernel functions and their relevant parameters give regression LS-SVM different generalization abilities. Establishing the optimal LS-SVM model is to determine the optimal Kernel function and its relevant parameters so as to minimize the test error of LS-SVM model. This procedure is also called model selection. As for the case of void fraction measurement in our context, for each kind of flow pattern of two-phase flow, we use linear Kernel function, polynomial Kernel function and radial Kernel function as the Kernel function of the void fraction measurement model in turn, and determine the relevant parameters. Finally, we test the model performance through the independent testing data set and select the model which has the best performance under each flow pattern for the practical void fraction measurement application.

In this work, the procedure for establishing the optimal void fraction model involves three aspects:
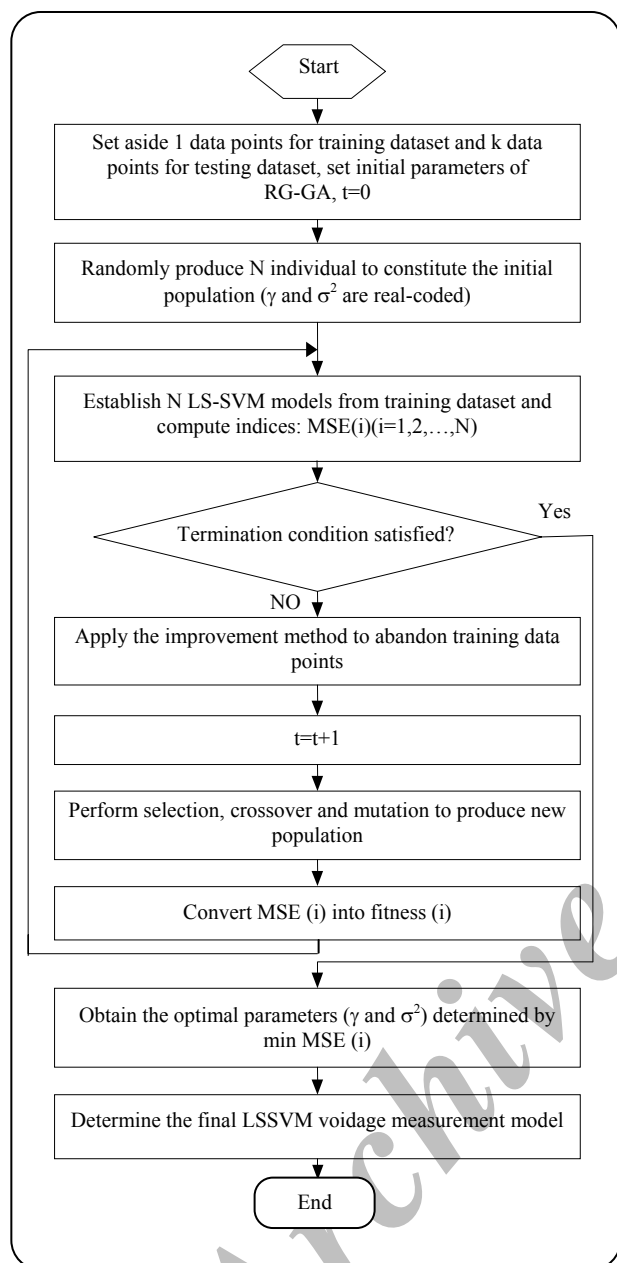
Fig. 8: Flow chart for void fraction measurement modeling.

the improvement of LS-SVM, the optimal selection of LS-SVM parameters and the selection of the Kernel function, as discussed above. The modeling process for void fraction measurement of two-phase flow is shown in Fig. 8. It is necessary to point out that we use the radial basis function as the Kernel function example in Fig. 8. The modeling procedures using the other Kernel functions are similar to that in Fig. 8.

RESULTS AND DISCUSSION

Because of the lack of any dynamic measurement method for the true void fraction value of two-phase flow, experiments were carried out by static experimental data to verify our proposed void fraction measurement method. Many void fraction measurement experiments of the three different cross-section flow patterns were conducted by simulating the two-phase flow. The media were diesel oil and air. The relative dielectric constant of oil is 2.56. The total data set was made up of 180 groups of data points from stratified flow, 169 from bubble flow and 120 from annular flow. According to the above modeling procedure of void fraction measurement, the optimal void fraction measurement model was established. The Kernel functions and their optimal parameters (regulation parameter γ and Kernel parameters) corresponding to different void fraction models under the three different flow patterns were obtained, as listed in Table 4. The maximum void fraction measurement errors (MaxE) under different flow patterns are also listed in Table 4. From Table 4, the maximum measurement errors are 3.9%, 5.3%, 4.4% corresponding to stratified flow, bubble flow, and annular flow, respectively. Fig. 9 shows the comparison between the measurement value of the void fraction and the actual void fraction value.

The research results show that the maximum error of void fraction measurement is 6% within the void fraction range from 10% to 90%. This can satisfy the field application requirements. Compared with the conventional void fraction measurement method based on image reconstruction, the new method omits the complex image reconstruction process and only needs a rough cross-section image reconstruction by a simple and quick back projection algorithm to obtain qualitative flow pattern information. Thus, the new method is characterized by simple computation. The measurement time is within 0.08 s. The real time performance is greatly improved. Because of adapting multiple void fraction measurement models for the different flow patterns, the new method effectively overcomes the influence of flow patterns on the void fraction measurement.

CONCLUSIONS

Compared with commonly used void fraction methods based on ECT, the proposed method effectively overcomes

48

Table 4: Kernel functions and their parameters of void fraction models at three different flow patterns.

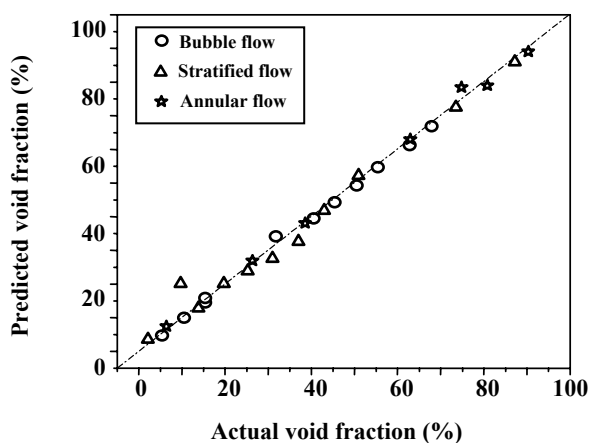| Flow pattern	$K\left(C_r, C_{ri}\right)$	Kernel parameters	γ	MaxE / %
Stratified flow	$\exp\left(\dfrac{-\left\|C_r - C_{ri}\right\|^2}{\sigma^2}\right)$	$\sigma^2 = 26$	2.1	3.9
Bubble flow	$\exp\left(\dfrac{-\left\|C_r - C_{ri}\right\|^2}{\sigma^2}\right)$	$\sigma^2 = 42$	5.8	5.3
Annular flow	$\left(C_r\right)^T C_{ri}$	—	0.5	4.4

Fig. 9: Experimental results.

the influence of flow patterns on the void fraction measurement results by invoking the LS-SVM void fraction model corresponding to a certain flow-pattern. Compared with the previous time-consuming image reconstruction model, the real-time performance is greatly improved and the measurement time is only 0.08 s.

Also, an easy, sparser, LS-SVM is proposed. This simplifies the mode structure of LS-SVM and improves the robustness of the LS-SVM model. We regard the LS-SVM parameter selection as an optimization problem. By virtue of the strong global searching ability of RC-GA, the optimal parameter combination is determined. This parameter optimization method possesses the universality.

Acknowledgments

Nomenclatures

l	The number of training data points
α	Void fraction value
β_i	The coefficient of support vectors
γ	Regulation parameter
γ_{lower}	The upper bound of γ
σ^2_{lower}	The lower bound of σ^2
C	Capacitance measurement value
σ	Parameter of radial basis Kernel function
b	Bias term
MSE	Mean Square Error

REFERENCES

[1] Hewitt G.F., "Measurement of two phase flow parameters", Academic Press, London, (1978).

[2] Huang Z.Y., Wang B.L. and Li H. Q., Application of Electrical Capacitance Tomography to the Void Fraction Measurement of Two-Phase Flow, *IEEE Transactions on Instrumentation and Measurement*, **52** ,p. 7 (2003).

[3] Vapnik V.N., "Statistical learning theory", Wiley, New York, (1998).

[4] Suykens J.A.K. and Vandwalle J., Least Squares Support Vector Machine Classifiers, *Neural Processing Letters*, **9**, p. 290 (1999).

[5] Cao L.J. and H Tay F.E., Support Vector Machine with Adaptive Parameters in Financial Time Series Forecasting, *IEEE Transactions on neural networks*, **14**, p. 1506 (2003).

49

[6] Wang B.L., Ji H.F., Huang Z.Y., Li H.Q., A High-Speed Data Acquisition System for ECT Based on the Differential Sampling Method, *IEEE Sensors Journal*, **5**, p. 308 (2005).

[7] Xie D.L., Huang Z.Y., Ji H.F., Li H.Q., An Online Flow Pattern Identification System for Gas-Oil Two-Phase Flow Using Electrical Capacitance Tomography. IEEE Trans., *Instrum. Meas.,* **55**, p. 1833 (2006)

[8] Suykens J.A.K., De Brabanter J., Lukas L., Vandewalle J., Weighted Least Squares Support Vector Machines: Robustness and Sparse Approximation, *Neurocomputing*, **48**, p. 85 (2002).

[9] Chapelle O., Vapnik V.N., Bousquet O., Mukherjee S., Choosing Multiple Parameters for Support Vector Machines, *Machine Learning*, **46**, p.131 (2002).

[10] Michalewicz, Z., "Genetic Algorithms + Data Structures = Evolution Programs**",** Springer, Verlag (1992).

[11] Chuang C.C., Su S.F., Robust Support Vector Regression Networks for Function Approximation with Outliers, *IEEE Transaction on Neural Networks*, **13**, P. 1322 (2002).

[12] Hwang J.N., Martin S.H., Martin M. R., Schimer J., Regression Modeling in Back-Propagation and Projection Pursuit Learning, *IEEE Transactions on Neural Network*, **5**, p. 342 (1994).